

WING DESIGN FOR WIND TUNNEL FLUTTER TESTING

Ulf Ringertz¹

¹Department of Aeronautical and Vehicle Engineering
Kungliga Tekniska Högskolan (KTH), Stockholm, Sweden

Keywords: Transonic, wind tunnel, flutter, aeroelasticity

Abstract: The design, analysis and structural testing of a new wing for a flutter wind tunnel model is considered. The aircraft configuration represents a modern light weight fighter configuration with external stores. A first test in the Transonic Dynamics Tunnel (TDT) at NASA Langley was performed in 2016 and the upcoming second test is planned for 2020.

During the first test program, a large amount of static aeroelastic data was acquired both in air and heavy gas (R134a) and also some dynamic data. Flutter testing was also performed but only two flutter conditions were achieved before model damage.

For the second test, a new wing structural design is being developed in order to allow flutter testing also without under-wing external stores and without significant mass balancing. However, in order to maintain sufficient structural strength, design optimization is required. The new design is to maintain the same strength as the first design tested but with much lower flutter dynamic pressure in transonic conditions. The strength requirements are considered using structural testing in combination with linear elastic finite element analysis.

The design process has demonstrated that changing the composite layup will have a very significant influence on the predicted flutter dynamic pressure without loss of strength. By using a mix of glass-fiber weave with a few layers of uni-directional glass-fiber and tailoring of the fiber orientation, a sufficiently large reduction in flutter dynamic pressure can be obtained.

1 INTRODUCTION

An aeroelastic wind tunnel model was designed and built at KTH for testing in the Transonic Dynamics Tunnel (TDT) at NASA Langley [1]. A first test program was performed during the summer of 2016 and preparations are now in progress for a second test in 2020. The wind tunnel model represents a modern light weight fighter configuration with external stores, as shown in Figure 1.

The model has an internal data acquisition and control system [2] mounted in the fuselage and data is streamed to the wind tunnel control room using fiber optic Ethernet communications. The model is instrumented with strain gauges, accelerometers, and



Figure 1: The model installed in the TDT test section.

wing surface pressure taps. An optical motion capture system [3] is used to accurately measure model deformation during testing.

During the first test program, a large amount of static aeroelastic data was acquired both in air and heavy gas (R134a) and also some dynamic data from model excitation using internal shakers and rapid motion of the canards. Finally, flutter testing was performed but only two flutter conditions were achieved before model damage. At the second flutter point, the wing deformation amplitude grew very quickly resulting in damage to the wing skins at both wing tips. Fortunately, no model parts broke away thus avoiding any foreign object damage to the wind tunnel.

The wing design for the first test was very conservative with the main goal to achieve a very strong wing structure satisfying the rather strict NASA requirements [4] for strength. In order to achieve flutter it was necessary to perform mass balancing to the wing tips to bring down the flutter dynamic pressure. This mass balance unfortunately also led to large inertial forces on the outer wing panel at the second flutter point.

2 MODIFIED WING STRUCTURAL DESIGN

Testing in NASA's large scale wind tunnel facilities requires that the model has to be rather thoroughly tested and analyzed before wind tunnel testing can be performed. Only numerical analysis of structural strength is not sufficient meaning that all critical components also have to be tested by proof-loading.

Structural analysis is performed using the rather detailed finite element model (FEM) shown in Figure 2. Static loads are obtained using computational fluid dynamics (CFD) [5,6] based on solving the Euler equations for a large number of cases. Several transonic Mach numbers are considered and the angle of attack and angle of side slip are allowed to be up to 5 degrees at the maximum dynamic pressure of approximately 10 kPa (200 psf). Following NASA requirements [4], the model should sustain these loads with a safety factor of 3 giving an ultimate loading on each wing panel of approximately 5000

Newtons.

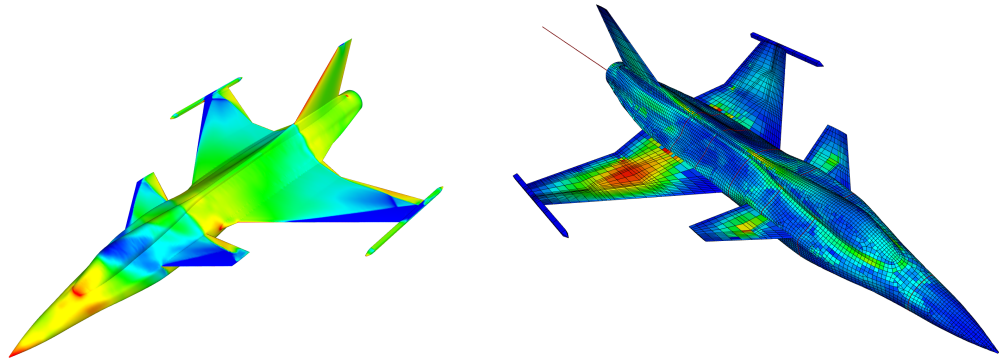


Figure 2: Highest loads at Mach 0.95, $\alpha = 5$ deg and $\beta = 5$ deg.

Flutter predictions are obtained using standard doublet lattice modeling (DLM) to allow rapid predictions for a large number of cases. The design optimization is simply performed by analyzing a large number of design cases with different layup of the composite wing skin. Static analysis is performed for each design to check that maximum local strain is below the required limit which in this case is 1% maximum strain.

For the second test, a new wing structural design is being developed in order to allow flutter testing also without under-wing external stores and without significant mass balancing. However, in order to maintain sufficient structural strength, design optimization is required.

The wing structural concept consists of a sandwich structure with Divinycell foam core [7] and thin epoxy fiber-glass composite wing skins. An internal skeleton structure is placed in the wing mid-plane to support concentrated forces from pylons and external stores. The original wing skin composite layup was rather simple with 3 layers of fiber-glass weave at 200 gram/m². One layer was oriented with fibers parallel and perpendicular to the aircraft plane of symmetry and an additional layer with fibers oriented parallel and perpendicular to the wing leading edge (# × #).

The new design is to maintain the same strength as the first design tested but with much lower flutter dynamic pressure in transonic conditions. The strength requirements are considered using structural testing in combination with linear elastic finite element analysis. In order to reuse all computational models developed for the first test it is desirable to maintain the structural topology and only change the properties of the composite wing skins. The new wing skins have five layers with three layers of a thin 80 gram/m² weave and two layers of uni-directional fibers at 200 gram/m² aligned with an angle θ to the aircraft plane of symmetry. An automated procedure was set up to scan a large number of combination of the layers. After fixing the weave orientation to be parallel and perpendicular to the wing leading edge, the orientation of the uni-directional layers was varied in small steps giving the flutter dynamic pressure versus

orientation variable result shown in Figure 3. The variable θ was chosen to be 70 degrees since the resulting wing skin layup ($\times // \times // \times$) also satisfies the strength constraint of 1% maximum strain.

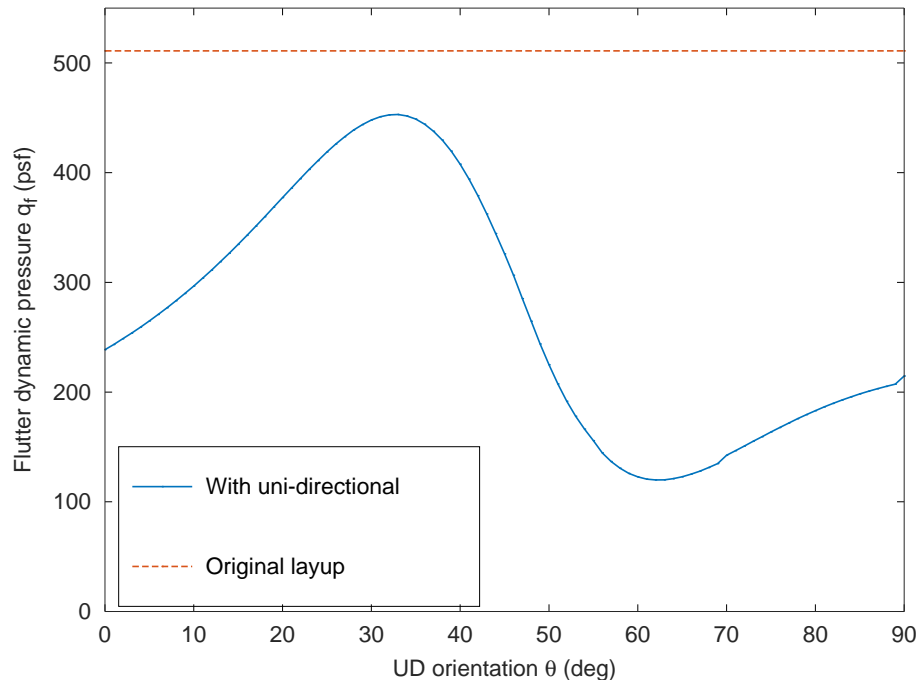


Figure 3: Predicted flutter dynamic pressure versus UD fiber direction.

The estimated drop in flutter dynamic pressure in this clean configuration with only the wing tip missiles is significant from slightly above 500 psf down to about 150 psf which is well within the TDT operating range.

3 WING MANUFACTURING

The wings are built using moulds obtained with a computer controlled milling machine using CAD data for the geometry. Reference holes for wing brackets and pylon attachments are also drilled through the moulds and hardened drill bushings are installed for precise location of these holes. A soft filler is used to plug the holes during the lamination process. An aluminum frame with double sided adhesive tape is used to accurately maintain fiber orientation as shown in Figure 4.

After placing the frame with weave on top of the mould, see Figure 5, resin is applied and the excess weave cut away so that the frame can be removed. When all the wing skin layers are applied, the core material is placed in the mould before the resin starts to cure. Also the core material has been milled to precise shape based on CAD geometry.

The entire mould with skins and sandwich core is then placed in a vacuum bag on top of a flat steel table. After curing the composite, excess core foam is milled away as shown in Figure 6.

Pressure taps are drilled through the wing surface using a template with drill bushings



Figure 4: Wing moulds and fiber placement.



Figure 5: Wetting out and placing core.



Figure 6: Vacuum bag and milling excess core.

installed, see Figure 7. The templates are obtained using 3D printing technology based on CAD geometry.

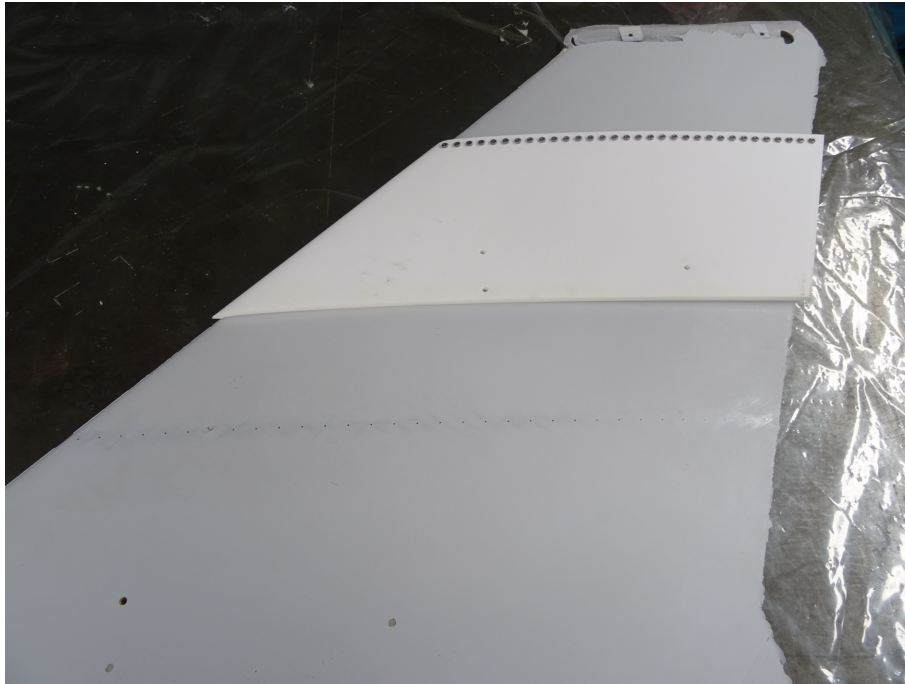


Figure 7: Drilling the pressure taps.

Finally, stainless steel tubes are installed, see Figure 8 close to the wing mid surface to minimize the structural stiffness contribution from the steel tubing. The tubing connects the pressure tap to the pressure scanners installed in the fuselage of the model.



Figure 8: Installation of tubing and ready for final assembly.

In the final step, the internal skeleton shown in Figure 4 is placed between the upper and lower wing skin with foam and the whole structure glued together to form a complete wing structure.

4 STRUCTURAL TESTING

The quality of the FEM is checked by applying point loading in the local hard points and comparing the computed deformations with the deformations measured using the optical motion capture system as shown in Figure 9.



Figure 9: The structural stiffness testing.

The stiffness check is followed by proof-loading with 3 times design load at $q=10$ kPa (200psf) or approximately 500 kg on each wing panel. The new wing design is slightly stiffer compared to the previous design as shown in Figure 10. There is also some

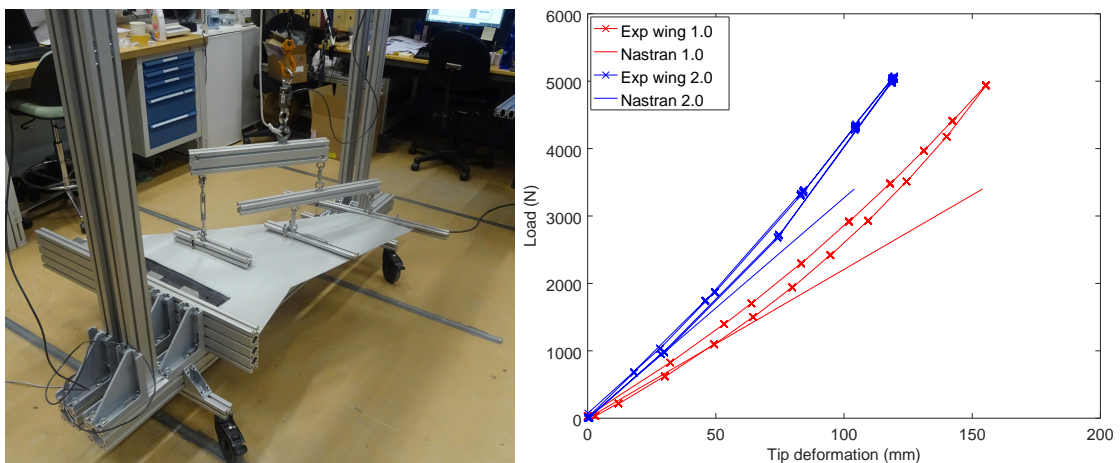


Figure 10: Proof loading the new wing structural design.

geometrically nonlinear effect in the proof-load test but repeated loading revealed no

permanent damage at loads up to the required ultimate loading.

Structural testing is also performed on structural components, such as the wing bracket interfacing the wing to the fuselage, and the external stores with pylons and attachments.

5 DATA SYNCHRONIZATION

A significant effort is currently in progress concerning synchronization of the data acquired during testing. The main data obtained can be essentially be divided in three different groups

1. Accelerometers, strain gauges, load cells, pressure transducers
2. Unsteady pressure scanner measurements
3. Position of markers using a motion capture system

The first group consists of traditional analog measurements that are acquired either by on board systems [2] or using the TDT AB-BAS system [8] which perform signal conditioning and conversion to digital data before storage. The second group of data is obtained using a dedicated pressure measurement system [9,10] based on a control unit and miniature pressure scanners that are located in the fuselage of the model. Data is almost acquired simultaneously for all pressure channels but some multiplexing is also involved as discussed in detail by Jansson and Stenfelt [11]. The third group of data is obtained by a motion capture system [3] which is based on a set of digital cameras that track the position of passive or active LED markers. Determining the position of each marker in three-dimensional space requires some processing meaning that data is not immediately available. The delay is small but significant for unsteady testing.

In the first round of testing in 2016 [6], data from the different system were acquired and synchronized using a trigger for simultaneous start and then a TTL signal was distributed as a reference for synchronization of the data. All data from the different systems were streamed over high-speed Ethernet using either TCP/IP or UDP protocols [12].

However, postprocessing to ensure accurate synchronization proved difficult due to the various delays between actual physical data and when data was actually available and stored. The different systems also acquired data at different rates due to limitations in each system. For the next testing, currently planned for 2020, better procedures for data synchronization are desired.

5.1 Precision time protocol

An alternative to trying to use signal based synchronization using triggers and reference signals is to use the Precision Time Protocol (PTP) which is an international standard (IEEE-1588) [13]. Using PTP means that no direct signals are needed for synchronization between various data acquisition systems. Instead, synchronization is based on making sure that all systems involved use the same time reference and that all data is time stamped when acquired rather than when stored.

With hardware support for PTP it is possible to achieve very high accuracy with differences in time less than a microsecond. To achieve this level of accuracy, some upgrades have been necessary. First, a so called grand master clock is used to define the time. In the present case this is provided using a special GPS satellite receiver [14]. The systems participating in the Ethernet network are attached to PTP enabled Ethernet switches and each system clock is adjusted continuously to maintain accurate time using the PTP protocol. The system also allows for having multiple GPS receivers to ensure redundancy and the participating systems automatically find the most accurate time reference using the so-called *Best Master Clock Algorithm* which is part of PTP.

To achieve best possible performance using PTP several data systems have been replaced. The on-board data acquisition system has been upgraded to the most recent version [15] which supports PTP also in hardware. The camera system [3] also supports PTP after a software upgrade. However, the pressure scanner system [9, 10] does presently not support PTP. Fortunately, the pressure system allows for each data sample to be triggered from an outside source. In the present implementation, the pressure system is triggered using a separate PXI system with a special time keeping module [16] making it possible to precisely time stamp each pressure measurement. Testing is currently in progress to establish the quality and possible uncertainties in the synchronization of the different data acquisition systems.

An illustration of the synchronization accuracy is shown in Figure 11. An accelerometer is placed at the wing tip of a wing installed in the low-speed wind tunnel at KTH. An optical marker is placed on top of the accelerometer and the structure is then excited using a shaker running at 12 Hz. The graph shows the acceleration as measured by the accelerometer but also the amplitude of the displacement of the marker times frequency squared obtained from the optical camera system. Some difference in amplitude

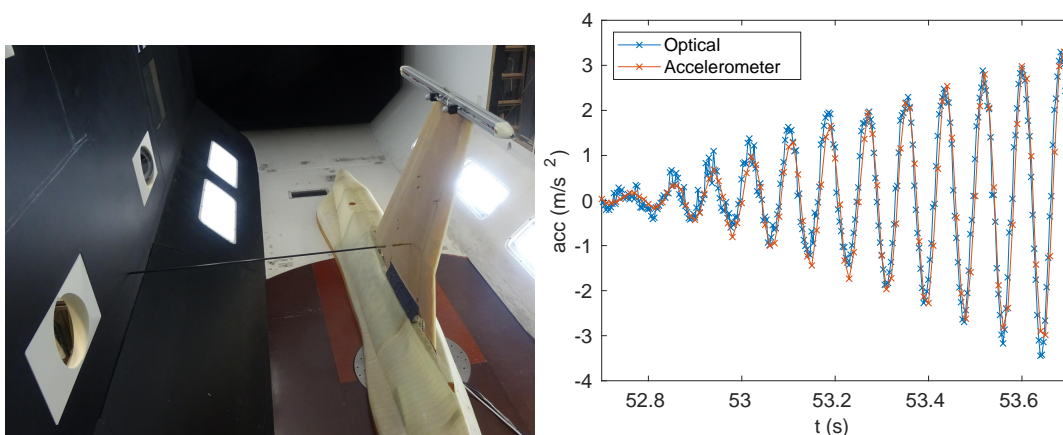


Figure 11: Comparing measured acceleration with second derivative of deformation.

is visible but the difference in time is less than the inverse of sampling rate of the accelerometer which is 2 kHz in this case. This clearly demonstrates the power of using PTP since the only common signal for these two measurements is the common GPS time source.

6 CONCLUSION

The design process has demonstrated that changing the composite layup will have a very significant influence on the predicted flutter dynamic pressure without loss of strength. By using a mix of glass-fiber weave with a few layers of uni-directional glass-fiber and tailoring of the fiber orientation, a sufficiently large reduction in flutter dynamic pressure can be obtained.

A first wing panel using the new optimized composite layup has been built and is currently being tested for stiffness and strength properties. Following these tests, vibration testing will be performed and the finite element adjusted to match the experimental data as best as possible using only minor adjustments of the composite layup data in the finite element model of the wing skins.

In conclusion it appears that it is possible to design a new wing skin layup with sufficient strength and sufficiently low flutter dynamic pressure. Further, only small changes of the material properties cards of the FEM are needed for an accurate representation of the real wing structure to be tested in the wind tunnel.

ACKNOWLEDGMENTS

This effort is financially supported by the Swedish Defense Materiel Administration (FMV) project number 416043-LB936757 monitored by Curt Eidefeldt and Erik Prisell.

7 REFERENCES

- [1] NASA Langley Research Center, www.aeronautics.nasa.gov/atp (2009). *Transonic Dynamics Tunnel*. Fact sheet.
- [2] National Instruments (2016). *NI cRIO-9068 User manual*. Document 376007B-03, www.ni.com.
- [3] Qualisys AB. *Oqus - Qualisys motion capture camera with high-speed video*. Product Information 100, 300 and 500 series, 2011.
- [4] NASA Langley Research Center, Langley Management System (LMS) (2015). *Wind-tunnel model systems criteria*, LPR 1710.15J ed. Expires April 30, 2020.
- [5] Eliasson, P. (2002). EDGE, a Navier-Stokes solver for unstructured grids. *Proc. to Finite Volumes for Complex Applications III*, ISBN, 1(9039), 9634.
- [6] Ringertz, U., Eller, D., Keller, D., et al. (2017). Design and testing of a full span aeroelastic wind tunnel model. In *Proceedings of International Forum on Aeroelasticity and Structural Dynamics*. Como, Italy. IFASD-2017-169.
- [7] Group, D. *Divinycell H The high performance sandwich core*. Data sheet, Doc No H June 2015 rev15 SI, www.diabgroup.com.
- [8] Ivanco, T., Sekula, M., Piatak, D., et al. (2016). A new high channel-count, high scan-rate, data acquisition system for the NASA Langley Transonic Dynamics Tunnel. In *54th AIAA Aerospace Sciences Meeting*, no. AIAA 2016-1149 in AIAA SciTech Forum and Exposition.

- [9] (2014). *Optimus Pressure Scanning System*. Data sheet, www.meas-spec.com or www.te.com.
- [10] Measurement specialties (2012). *DTC Initium Networkable wind tunnel electronic pressure scanning*. Data sheet, www.meas-spec.com.
- [11] Jansson, N. and Stenfelt, G. (2014). Steady and unsteady pressure measurements on a swept-wing aircraft. *The Aeronautical Journal* (1968), 118(1200), 109–122. doi:10.1017/S0001924000009015.
- [12] Stevens, W. R. (1997). *UNIX Network Programming: Networking APIs: Sockets and XTI*. Upper Saddle River, NJ, USA: Prentice Hall PTR, 2nd ed. ISBN 013490012X.
- [13] IEEE Instrumentation and Measurement Society, www.ieee.org (2008). *1588-2008 - IEEE Standard for a Precision Clock Synchronization Protocol for Networked Measurement and Control Systems*, 1588-2008 ed.
- [14] (2017). IGM-1100 Portfolio User Guide. www.microsemi.com.
- [15] National Instruments (2018). *NI cRIO-9048 Specifications*. Document 376785F-02, www.ni.com.
- [16] National Instruments (2017). *NI PXI-6683 Series User Manual*. [Www.ni.com](http://www.ni.com).

COPYRIGHT STATEMENT

The authors confirm that they, and/or their company or organization, hold copyright on all of the original material included in this paper. The authors also confirm that they have obtained permission, from the copyright holder of any third party material included in this paper, to publish it as part of their paper. The authors confirm that they give permission, or have obtained permission from the copyright holder of this paper, for the publication and distribution of this paper as part of the IFASD-2019 proceedings or as individual off-prints from the proceedings.